

**STUDY ON THE EFFECT OF MnO₂ AS SINTERING ADDITIVE IN STRUCTURAL,
MAGNETIC AND ELECTRICAL PROPERTIES OF SOLID-STATE DERIVED
Ni_{0.8}Zn_{0.2}Fe₂O₄**

A THESIS SUBMITTED IN PARTIAL FULFILLMENT
OF THE REQUIREMENTS FOR THE DEGREE OF
BACHELOR OF TECHNOLOGY
IN CERAMIC ENGINEERING

BY
VIVEK SHARMA
111CR0510



DEPARTMENT OF CERAMIC ENGINEERING
NATIONAL INSTITUTE OF TECHNOLOGY
ROURKELA - 769008
2014-15

**STUDY ON THE EFFECT OF MnO₂ AS SINTERING ADDITIVE IN STRUCTURAL,
MAGNETIC AND ELECTRICAL PROPERTIES OF SOLID-STATE DERIVED
Ni_{0.8}Zn_{0.2}Fe₂O₄**

A THESIS SUBMITTED IN PARTIAL FULFILLMENT
OF THE REQUIREMENTS FOR THE DEGREE OF
**BACHELOR OF TECHNOLOGY
IN CERAMIC ENGINEERING**

BY
VIVEK SHARMA
111CR0510

Under the guidance of

Prof. Arun Chowdhury



**DEPARTMENT OF CERAMIC ENGINEERING
NATIONAL INSTITUTE OF TECHNOLOGY
ROURKELA – 769008
2014-15**



National Institute of Technology, Rourkela

CERTIFICATE

This is to certify that the thesis entitled "Study on the effect of MnO_2 as sintering additive in structural, magnetic and electrical properties of solid-state derived $Ni_{0.5}Zn_{0.5}Fe_2O_4$ " submitted by Vivek Sharma (Roll No. 111CR0510) in partial fulfilment of the requirements for the award of Bachelor of Technology degree in Ceramic Engineering at the National Institute of Technology, Rourkela is an authentic work carried out by him under my supervision and guidance.

To the best of my knowledge, the matter embodied in this thesis has not formed the basis for the award of any Degree or Diploma or similar title of any University or Institution.

Arun Chowdhury

Arun Chowdhury

Assistant Professor

Ceramic Engineering Department

NIT, Rourkela-769008

Date:

ACKNOWLEDGEMENT

I would like to express my profound gratitude and indebtedness to Prof. Arun Chowdhury, Ceramic Engineering Department, NIT Rourkela for his guidance and valuable suggestions. This work would not have been possible without his encouragement and constructive criticism. I sincerely thank him for the time and patience he devoted for this work. I am indebted to HOD of the Depart. Of Ceramic Engineering for encouraging me at my project work and for providing the departmental facilities. I would like to pay my sincere thanks to Director and all technical assistant at various laboratory in this institute.

I am also thankful to all the faculty members for their valuable suggestions.

I am immensely thankful to all technical and officers of the department and especially to Arvind Sir and Bapi Sir for their help in carrying out laboratory experiments.

I would like to acknowledge the authors of different research paper referred in the work, which were a valuable source for understanding the subject.

Lastly, I am thankful to all my friends who encouraged and helped me in accomplishing this project.

Vivek Sharma
111CR0510
Department of Ceramic Engineering
NIT Rourkela

ABSTRACT

Ni-Zn ferrites have been synthesized with varying MnO_2 as sintering aid as well as enhancer in magnetic property. The influence of MnO_2 additive on the properties of Ni-Zn ferrites was studied by the conventional ceramic method (solid oxide mixing followed by calcination). The results showed that MnO_2 does not form a visible second phase while the added concentration was restricted to 0–0.6 weight%. The average grain size, sintering density and gradually decrease with the increase of the MnO_2 content. And the DC resistivity continuously increases with the increase of MnO_2 content. The saturation magnetization (magnetic moment in unit mass) first increases slightly when mass fraction of MnO_2 is less than 0.4% MnO_2 , and then gradually decreases with increasing the MnO_2 mass fraction due to the exchange interaction of the cations. When the excitation frequency is less than 1 MHz, the power loss (P_{cv}) continuously increases with increasing the MnO_2 content due to the decrease of average grain size. However, when the excitation frequency exceeds 1 MHz, eddy current loss gradually becomes the predominant contribution to P_{cv} . The present investigations reports the effect of additive MnO_2 in varying amount i.e. 0.0%, 0.2%, 0.4% and 0.6% on the structural, magnetic and electric properties of $\text{Ni}_{0.8}\text{Zn}_{0.2}\text{Fe}_2\text{O}_4$ prepared by solid oxide mixing method. The powders were calcined at 950°C for 4hrs, XRD analysis conducted. After the confirmation of phases, powders were pressed into pellet. The pellet of different composition were sintered at different temperature and characterized for apparent porosity, bulk density and B-H loop using Magneta. For the phase formation, the pellets were characterized by using XRD and for the microstructure analysis, the pellets were characterized by using FESEM. DC resistivity, magnetic properties are affected by addition of MnO_2 .

Table of Contents

<i>ITEMS</i>	<i>TOPICS</i>	<i>PAGE NO.</i>
<i>a.</i>	Certificate	1
<i>b.</i>	Acknowledgement	2
<i>c.</i>	Abstract	3
<i>d.</i>	Table of contents	4
<i>e.</i>	List of figures	5
<i>f.</i>	List of tables	6
<i>1.</i>	Introduction	7
<i>2.</i>	Literature Review	11
<i>3</i>	Experimental Procedure	16
<i>3.1</i>	Solid oxide mixing method for the preparation of $\text{Ni}_{0.8}\text{Zn}_{0.2}\text{Fe}_2\text{O}_4$	17
<i>3.1.6</i>	Synthesis of ferrite powder and pellets	20
<i>3.2</i>	Characterization	21
<i>4</i>	Result and Discussion	23
<i>4.1</i>	Structural Characterization	24
<i>4.1.1</i>	X-Ray Diffraction Analysis (XRD)	24
<i>4.2.2</i>	Microstructural Characterization	27
<i>4.3</i>	Bulk Density (B.D.)	35
<i>4.4</i>	Magnetic and Electric Properties	36
<i>5</i>	Conclusion	39
<i>6</i>	Reference	41

List of figures

Fig. No.	Pg. No.	DESCRIPTION
1.1	8	Unit cell of Ni-Zn Ferrite
1.2	9	Saturation Magnetization per formula unit for the ferrite $(\text{Fe}^{3+}_{1-\alpha}\text{Zn}^{2+\alpha})(\text{Fe}^{3+}_{1+\alpha}\text{Ni}^{2+}_{1-\alpha})\text{O}_4$
2.1	13	Permeability values of samples with different MnO ₂ mass Fractions
2.2	15	Hysteresis loops for Ni _{0.8} Zn _{0.2} Fe ₂ O ₄ at room temperature
3.1	20	Flow chart for the synthesis of Nickel Zinc Ferrite
4.1	24	XRD of calcined powder of batches containing (i)NZF+0.0MnO ₂ (ii) NZF+0.2MnO ₂ (iii) NZF+0.4MnO ₂ (iv) NZF+0.6MnO ₂
4.2	26	XRD of sintered pellets (i)NZF+0.0MnO ₂ (ii) NZF+0.2MnO ₂ (iii) NZF+0.4MnO ₂ (iv) NZF+0.6MnO ₂
4.3	28	Microstructure of compositions of Ni _{0.8} Zn _{0.2} Fe ₂ O ₄ sintered at 1200 °C for 4hr
4.4	30	Elemental mapping of NZF with 0.2 weight percentage MnO ₂ additive sintered at 1200 °C/4hr
4.5	31	Elemental mapping of NZF with 0.6 weight percentage MnO ₂ additive sintered at 1200 °C/4hr
4.6	32	Microstructures of all four compositions of NZF sintered at 1225 °C
4.7	34	Microstructures of all four compositions of NZF sintered at 1225 °C/2hr (inert atmosphere)
4.8	37	B-H loop at 1225 °C for 2 hours

List of Tables

Table no.	Page No.	DESCRIPTION
3.1	17	Amount of Additive and Ni-Zn ferrite in different composition
3.2	19	Firing schedule and sintering temperature
4.1	25	Table containing d-spacing, (hkl) plane and FWHM of calcined powder
4.2	27	Table containing d-spacing, (hkl) plane of sintered pellets
4.3	27	Crystallite size as per composition sintering temperature = 1225 °C; dwell time = 4hr
4.4	29	Average grain size of all four compositions sintered at 1200 °C for 4 hours:
4.5	33	Average grain size of all four compositions sintered at 1225 °C for 2 hours
4.6	35	Bulk density and apparent porosity value with % theoretical density of the ferrite having composition as Ni _{0.8} Zn _{0.2} Fe ₂ O ₄ , and Ni _{0.8} Zn _{0.2} Fe ₂ O ₄ with MnO ₂ in different amount as additive at 1200 °C for 4 hour
4.7	36	Bulk density and apparent porosity value with % theoretical density of the ferrite having composition as Ni _{0.8} Zn _{0.2} Fe ₂ O ₄ and Ni _{0.8} Zn _{0.2} Fe ₂ O ₄ +varying MnO ₂ as additive at 1225 °C for 2 hour
4.8	36	Bulk density and apparent porosity value with % theoretical density of the ferrite having composition as Ni _{0.8} Zn _{0.2} Fe ₂ O ₄ fired at 1225 °C for 4 hr
4.9	38	Hysteresis parameters of Ni _{0.8} Zn _{0.2} Fe ₂ O ₄ sintered at 1225 °C for 2 hours

CHAPTER 1

INTRODUCTION

Ferromagnetic materials are magnetic ceramics which are used for making many devices such as permanent magnets, memory storing devices, and microwave machines and for the telecommunication machines purpose. Spinel ferrites have been researched for their magnetic and electrical properties. Zn ferrite is a normal ferrite, whereas Ni ferrite is an inverse spinel. Therefore NiZn Ferrite is mixed spinel ferrite in which A-sites (tetrahedral) are occupied by Zn^{+2} and Fe^{+3} and B-sites (octahedral sites) are occupied by Ni^{+2} and Fe^{+3} ions. NiZn ferrite is a spinel ferrite. Magnetic spinels have the general formula $MO.Fe_2O_3$ or MFe_2O_4 where, M is divalent metal ion like Mn, Zn, Ni, Fe, or Co (or a mixture of such ions). In the spinel crystal structure the oxygen ions form a cubic close-packed array in which two types of interstice occur, one coordinated tetrahedrally and the other octahedrally with oxygen ions. The cubic unit cell is large, having eight formula units and containing 64 tetrahedral and 32 octahedral sites, customarily designated A and B sites respectively; eight of the A sites and 16 of the B sites are occupied. The unit cell shown in Fig. 1.1 is seen to be made up of octants, four containing one type of structure (shaded) and four containing another (unshaded). In this representation some of the A-site cations lie at the corners and face-centre positions of the large cube; a tetrahedral and an octahedral site are shown. The close-packed layers of the oxygen ion lattice lie at right angles to the body diagonals of the cube. The arrows on the ions, representing directions of magnetic moments, indicate that the B-site ions have their moments directed antiparallel to those of A-site ions, illustrating the antiferromagnetic coupling[1].

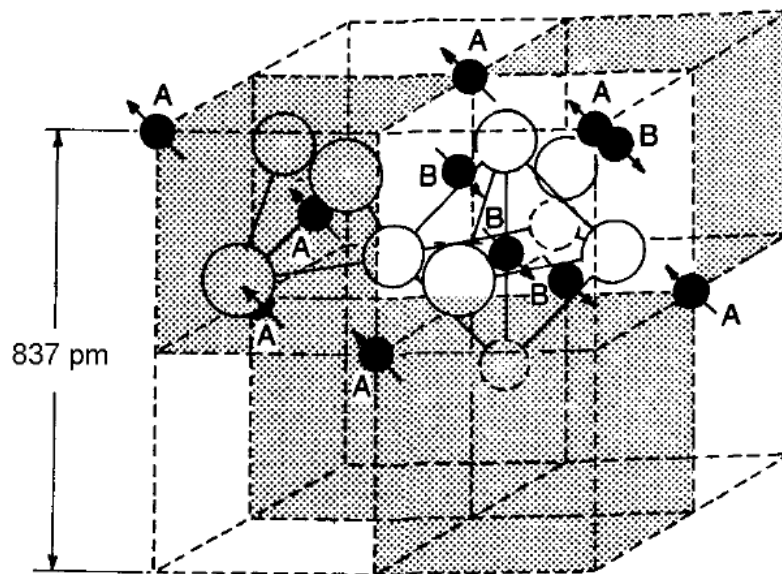


Fig1.1 Unit cell of Ni-Zn Ferrite

In a spinel structure, both divalent and trivalent cations are distributed among tetrahedral (A) and octahedral (B) sites. The site preference exhibited by divalent ions defines whether the spinel is normal, inverse or mixed. In normal spinel, the A^{2+} ions occupy only tetrahedral sites and the B^{3+} ions occupy only octahedral sites, for eg. $ZnFe_2O_4$. In inverse spinel, all the A^{2+} ions and half the B^{3+} ions sit on the octahedral sites; the tetrahedral sites are occupied now by the other half of the B^{3+} ions, for eg. $NiFe_2O_4$. In most cases, magnetic divalent cations (such as Ni^{2+}) prefer the octahedral sites and produce an inverse spinel structure. Diamagnetic divalent cations (such as Zn^{2+} , Cd^{2+}) have preference for the tetrahedral positions and the resulting structure is a normal spinel[2]. Therefore NiZn ferrite shows a mixed spinel structure.

Addition of a non-magnetic ion such as Zn to a spinel ferrite leads to an increase in saturation magnetization. The magnetic moment per formula unit MFe_2O_4 , where M represents Ni^{2+} or Zn^{2+} , is shown in Fig. 1.2 as a function of zinc substitution. Zinc ferrite is a normal spinel, indicating that Zn ions have a preference for the A sites, so that on substituting zinc for nickel the occupancy becomes $(Fe^{3+}_{1-\alpha}Zn^{2+}_{\alpha}) (Fe^{3+}_{1+\alpha}Ni^{2+}_{1-\alpha}) O_4$ in which the first and second brackets indicate occupancy of the A and B sub-lattices respectively. Thus the antiparallel coupling between moments on A and B sites is reduced because the occupancy of A sites by magnetic ions is reduced, and as a consequence the Curie point is lowered. However, the excess of moments on octahedral sites over those on tetrahedral sites is increased so that the magnetization is increased. The data plotted in Fig. 1.2 confirm this model up to $\delta \sim 0.4$. The fall in magnetization for higher values of δ is due to the reduced antiparallel coupling between the A and B sites, and it becomes zero when $\delta = 1$, i.e. $(Zn^{2+})(Fe^{3+})O_4$.

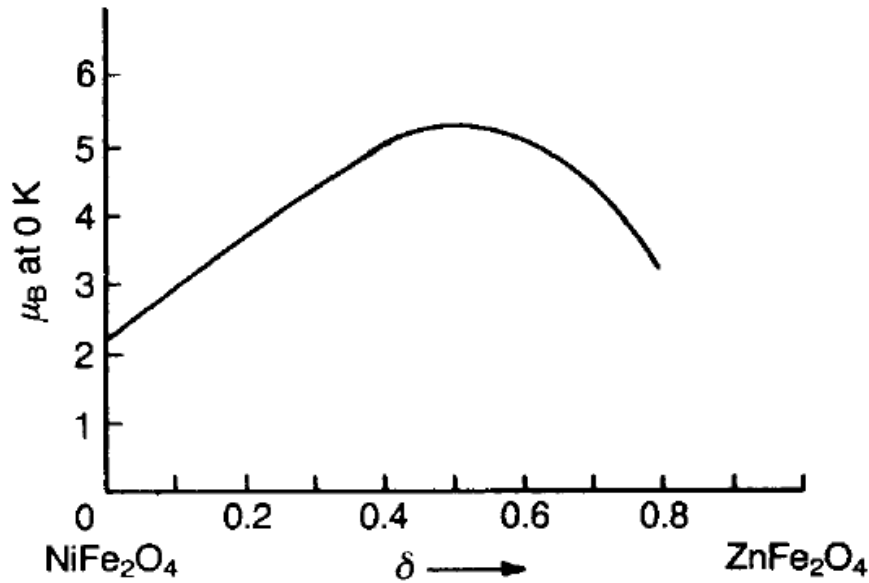
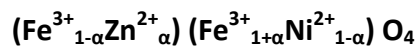


Fig. 1.2 Saturation Magnetisation per formula unit for the ferrite



Generally speaking, the spinel ferrites have low magnetic anisotropies and are magnetically ‘soft’; exceptions are those containing Co^{2+} which is itself strongly magnetically anisotropic. Cobalt spinel ferrites can have coercivities approaching 105Am^{-1} , placing them firmly in the ‘hard’ category[1].

Ni–Zn ferrites are one of the most versatile magnetic materials for general use, which have many applications in both low and high frequency devices and play a useful role in many technological applications such as microwave devices, rod antennas, read/write heads for high speed digital tape, cores for inductors, transformers and in switch mode power supplies etc. because of their high initial permeability, low magnetic losses, high resistivity, low dielectric losses, mechanical hardness, high Curie temperature and chemical stability[3,4].

CHAPTER 2

LITERATURE REVIEW

Nickel–zinc ferrites have excellent soft magnetic properties and are used in electronic and telecommunication industries. Ferrites are structure sensitive materials and their properties critically depend on the manufacturing process[5]. The densification of a pure NiZn ferrite to a sufficiently high density is difficult because of the relatively high melting point of some component oxides and low bulk diffusivity. As a result, it is very difficult to obtain a sintered body with density exceeding 90% of the theoretical density using solid state sintering.

In this section, review of the works carried out by many researchers on the synthesis of nickel zinc ferrites by different routes, impact of addition of different additives on the physical and magnetic properties of nickel zinc ferrites.

SU Hua et al. [6] reported the influence of MnO₂ additive on the properties of Ni-Zn ferrite formed by conventional powder metallurgy. The amount of MnO₂ varied from 0.0 to 2.0 % with the increase of 0.4%. After the experiments, it was concluded that MnO₂ does not form another visible phase in the range of 0-2% additive addition. The average grain size, permeability and sintering density of the Ni-ZN ferrite samples gradually decrease with the increase of MnO₂ content. But the DC resistivity continuously increases with increase of MnO₂ content. Talking about the magnetic properties, saturation magnetisation increases slightly in less than 0.4% additive addition, and then continuously decreases with the increase in MnO₂ content due to the exchange interaction of cations. When the excitation frequency is less than 1 MHz, the power loss (P_{cv}) increases with increasing the MnO₂ content because the average grain size decreases. However, when the excitation frequency exceeds 1 MHz, eddy current loss gradually becomes the predominant contribution to P_{cv} . And the lower P_{cv} is observed for the sample with higher resistivity, except for the sample with 2.0% MnO₂. Permeability variation can be observed from the below graph between permeability and frequency.

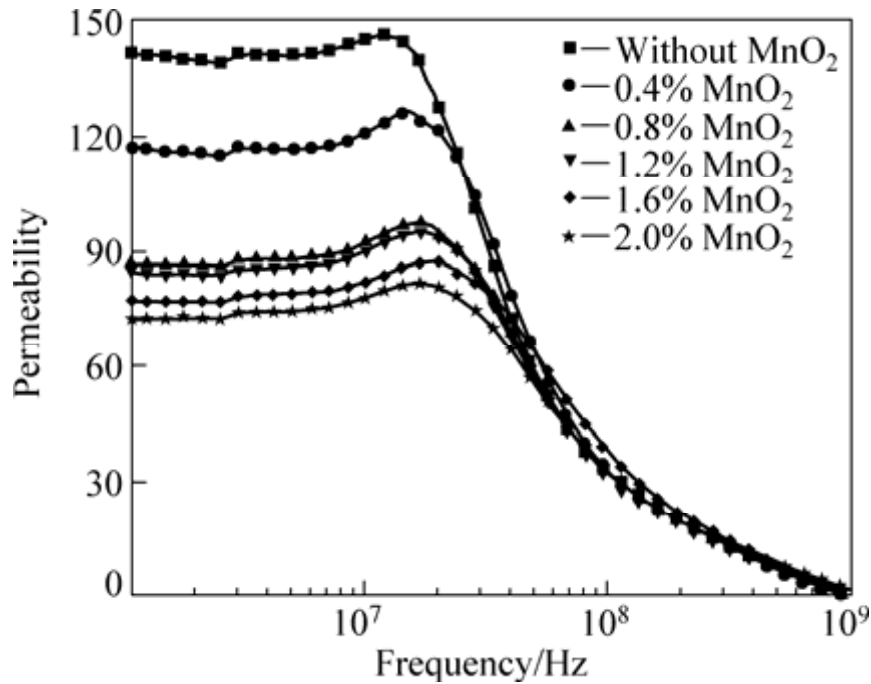


Fig.2.1 Permeability values of samples with different MnO₂ mass Fractions

S. S. Paik et al. [7] reported on the ferrite synthesis by different processing routes and magnetic properties of ferrite at various annealing temperature i.e. 800 °C, 900 °C, 1000 °C, and 1100 °C.

The manufacturing process used was dry method. The result shows that sintered sample at 1100 °C was having less amount of remaining powders and spinel peak is superior. Among the all 4 temperature variations, Ni-Zn ferrite was sintered most suitable at 1100 °C. From the SEM images, the size of the even particle of the sample which is sintered from below sintering temperature 1000 °C is below 1 μm, the size of the even particle of 2 hours sintered sample of 1100 °C is 3 μm. Magnetic properties of the samples sintered at 1000 °C for 2 hours is a ferri-magnetic M-T Curve and that Neel temperature assumed to be about 673 K. As the sintering temperature increases from 1000 °C to 1100 °C, residual induction decreases by 2.02 emu/g from 8.12 emu/g and coercive field decreases by 22.62 Oe from 54.23 Oe. But magnetization saturation increases by 73.31 emu/g in 59.64 emu/g, and the sample that sinters during 2 hours at 1000 °C and all samples that sinters during 2 hours at 1100 °C showed characteristics of soft magnetic material of low coercive coercivity and hysteresis curved areas are small. From the absorption area ratio, the tetrahedral sites diminished from 86.51 % by 30 % as the sintering temperature is increased, and the octahedral sites increases from 13.49 % by 70 %. It was also concluded from the results that all samples had two kinds of magnetic field directions.

Majid Niaz et al.[8] reported on the study of structural and magnetic characterization of Nano structured Ni_{0.8}Zn_{0.2}Fe₂O₄ prepared by self combustion method. The samples were sintered at 750 °C and 950 °C and characterization was carried out by XRD, SEM and Raman spectroscopy. The single phase and good nanoparticles of Ni_{0.8}Zn_{0.2}Fe₂O₄ were found at sintering temperature of 950 °C by analysing the X-Ray diffraction pattern. From the analysis of XRD and SEM, it was observed that particle size of the samples varied from 25 to 36 nm. It was found that with the increment in the temperature from 750 °C to 950 °C, grain size increases. At the sintering temperature of 950 °C, cubical shape microstructure of Ni_{0.8}Zn_{0.2}Fe₂O₄ was observed. The initial permeability was found to increase and relative loss factor decreased at high frequency. The powder sintered at 950 °C can be used for multilayer chip inductor and high frequency application due to ability to sinter at low temperature and low loss at high frequency.

Tania Jahanbin et al.[9] reported on the Influence of sintering temperature on the structural, magnetic and dielectric properties of Ni_{0.8}Zn_{0.2}Fe₂O₄ synthesized by co-precipitation route. In the process, the toroid and the pellet form samples were prepared and sintered at various temperatures from 700 °C to 1300 °C for 5 hours in steps of 200 °C. To find out the properties and their characterization, XRD, SEM and energy dispersive X-ray spectroscopy (EDXS) was performed. The dielectric and magnetic measurements were carried out using a vibrating sample magnetometer (VSM) and the impedance analyser, respectively. The highest density of 4.48 g cm⁻³ was found for the sample sintered at 1300 °C. It was observed that the RLF was in the order of 10⁻³ to 10⁻⁴ and the initial permeability increased from 4 to 17 in the frequency range of 1.0MHz to 1.0 GHz. Due to the high electrical resistivity, the RLF of the samples was low. The primary achievement of this report is the increment in operational frequency range over 400 MHz which is found at low sintering temperature (700 °C). The dielectric constant of all the samples decreases with increase in frequency.

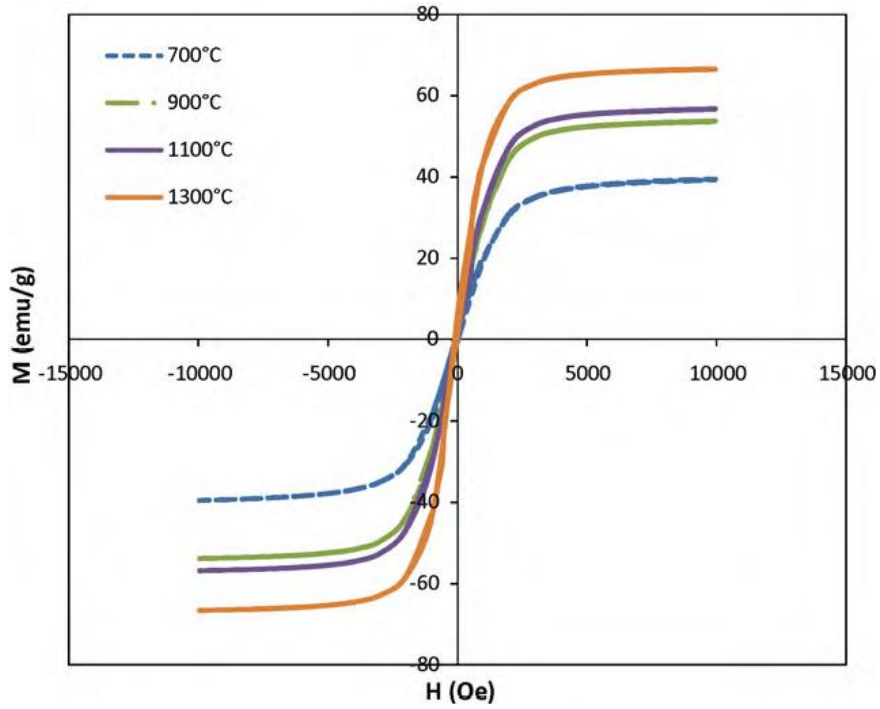


Fig. 2.2 Hysteresis loops for $\text{Ni}_{0.8}\text{Zn}_{0.2}\text{Fe}_2\text{O}_4$ at room temperature.

From the above graph, it was observed that the coercivity decreases by increasing the sintering temperature. This is because of the increase of the average grain size with sintering temperature

CHAPTER 3



EXPERIMENTAL

3.1 SOLID OXIDE MIXING METHOD FOR THE PREPARATION OF $\text{Ni}_{0.8}\text{Zn}_{0.2}\text{Fe}_2\text{O}_4$:

3.1.1 MIXING:

Nickel Oxide (NiO) having more than 98% purity, Zinc Oxide (ZnO) are weighed along with the Iron oxide (Fe_2O_3) of 98% purity in the fixed proportion of the chemical formula $\text{Ni}_{0.8}\text{Zn}_{0.2}\text{Fe}_2\text{O}_4$. The weighed raw materials are mixed together thoroughly to get the homogeneous mixture. Out of which, 50 gm of sample is taken in four plastic jar each and MnO_2 is added as a binder to the jar. 0%, 0.2%, 0.4%, 0.6% MnO_2 to the Jar 1, Jar 2, Jar 3 and Jar 4 respectively. Then iso-propanol was added in each jar for mixing because iso-propanol do not react with the composition taken. If water or any other solution were used instead of iso-propanol, that might react with the composition and may change the chemical properties of the composition. After adding iso-propanol to the all 4 compositions, shacked it very well to wet all the composition powder with the help of iso-propanol. And after that around 20 balls were put inside all the four compositions and then mixing process was carried out by pot milling for 24 hours. And then after 24 hours of homogenisation process, composition paste is taken in the Petridis and left for drying first in the air and the under the IR lamp. This whole process was carried for all the four compositions of NZF with different MnO_2 percentage.

For the comparison of properties with the addition of different amount of MnO_2 , 4 compositions were made with the same amount of NZF having different MnO_2 amount as additive.

Table: 3.1 Amount of Additive and Ni-Zn ferrite in different composition

Composition	MnO_2		$\text{Ni}_{0.8}\text{Zn}_{0.2}\text{Fe}_2\text{O}_4$
	Percentage (%)	Amount(gm)	
1	0.0	0.0	60
2	0.2	0.12	60
3	0.4	0.24	60
4	0.6	0.36	60

After pot milling by addition of iso-propanol in the four different compositions of powder for 24 hours, the paste was dried under the air and then under the IR lamp.

3.1.2 CALCINATION:

All the four samples with varying additive amount were calcined at 900 °C and 950 °C. Then the calcined powder were milled by adding acetone with the help of agate mortar to get the fine powder and then again dried the powder under IR lamp.

3.1.3 POWDER CHARACTERISATION:

Sample preparation and experimentation of powder XRD

XRD analysis was carried out to determine the phases present in the composition. X-Ray diffraction was performed with a Philip's Diffractometer (Model: PW-1830, Philips, Netherlands) to obtain the phases present in the calcined powder. After performing the X-Ray diffraction with the Philip's Diffractometer, a graph was plotted between X-Rays intensity against the angle Theta. The angle of each diffraction was converted to d-spacing by using the Bragg's Law i.e. $n\lambda = 2d \sin\theta$ (where 'n' is the order of diffraction and 'λ' is the wavelength of X-ray. For the identification of different phases present in the calcined powder, Philips X-pert high score software was used.

3.1.4 FORMING

After calcination of the powder samples and the phase confirmation, calcined powder of all 4 compositions was mixed thoroughly with 2 wt. % of binder i.e. polyvinyl alcohol with the help of agate mortar and pestle. In the starting, calcined powder of each composition were mixed with the PVA binder for approximately 1 hour. The powder mixed with PVA was then dried under the IR lamp. After the drying, nice granules of ferrite powder were produced where that granules having good flow ability and compressibility. After that, the granulated powders were uniaxially pressed at a load of 4 US Ton with the dwell time of 90 sec by using a hydraulic press to form a pellet of 10.5 mm diameter. Green density of the green pellet was calculated from weight/volume. From the green pellets, volume was calculated and weight was measured in the starting by using weighing balance. Then the sintering of green samples were performed by firing the pellets in an electric arc furnace at different temperatures.

3.1.5 SINTERING

Sintering was carried out in (1) an Electrical furnace (chamber furnace of highest temp. 1400 °C) with air atmosphere and in (2) an Electrically heated tube furnace with inert atmosphere. The details of firing schedule with sintering temperatures has been given in a table below:

Table: 3.2 Firing schedule and sintering temperature

Sintering	Binder burnt-out temperature	Temperature (°C)
1	600 °C/2hr	1200/4hr
2	600 °C/2hr	1225/2hr
3	600 °C/2hr	1225/4hr
4	600 °C/2hr	1250/2hr
5	600 °C/2hr	1225 (Ar Atmosphere)/2hr

3.1.6 Synthesis of ferrite powder and pellets:

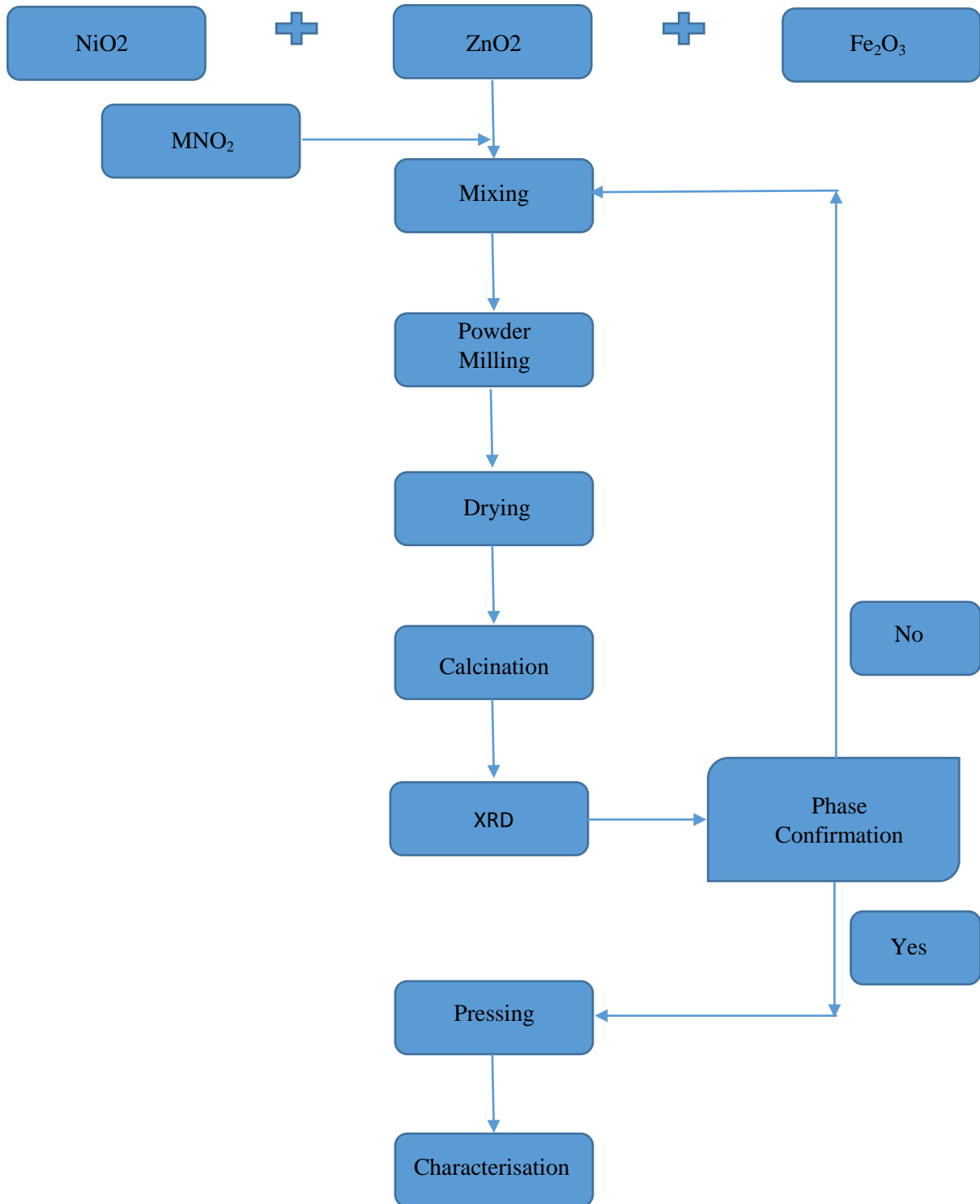


Fig3.1 Flow chart for the synthesis of Nickel Zinc Ferrite

3.2 Characterization

For the characterisation of sintered pellets, various physical properties of the sintered pellets such as bulk density, apparent porosity, phase analysis, microstructural analysis and magnetic properties such as B-H loop measurement were carried out for all the pellets of all 4 composition.

3.2.1 Phase Analysis:

X-Ray Diffraction was performed with a Philip's Diffractometer (model: PW-1830, Philips, Netherlands). The phase formation in the sintered pellets is studied and the phases present in the sample were identified by using the software called Philip's X-pert high score.

3.2.2 Bulk Density and Apparent Porosity:

Bulk density and apparent porosity of sintered pellets was found out by using the Archimedes principle. First, measured the dry weight of pellets by using the weighing balance. Then the sintered samples were kept in the beaker containing kerosene and kept in a vacuum chamber so that all the pores were filled up with kerosene completely. Beaker was kept in chamber for about 2 to 3 hours until the bubbling stops in the chamber. After that, Suspended weight and soaked weight of each pellet was measured using the electronic balance.

Apparent porosity and bulk density were calculated by using the formulas given below:

$$\text{Apparent porosity} = \frac{w-D}{W-S}$$

$$\text{Bulk density} = \frac{D}{W-S}$$

Where D = Dry wt. of the sample

S = Suspended wt. of the sample

W = Soaked wt. of the sample

3.2.3 Microstructural Analysis:

By using Scanning Electron Microscopy (SEM), the microstructure of the sintered pellets were identified. Firstly, before performing the SEM, the pellets were thinly coated by gold under vacuum condition so as to make the surface conducting for viewing through NOVA NANOSEM 450. The mounted samples were studied by SEM (JEOL- JSM 6480 LV). The Grain size of the pellets is found out by using the “Image J” software.

3.2.4 B-H Loop Measurement:

For the measurement of magnetic property, one “Magna Puls field magnetic loop tracer” was used. Before performing the measurement, dry weight and the volume of the samples were measured for the calibration. The “applied magnetic fields” were ranging from -6000 to +6000 Oe.

3.2.5. Electrical Resistivity Measurement

For the measurement of electrical resistivity, Agilent 34405A Digital Multimeter was used. By using the instrument, resistance was obtained for each composition of the pellet. Then, for calculating the resistivity, length and area of the pellet were measured and calculated by formula

$$R = \rho L / A$$

Where


R=Resistance

ρ = resistivity

L= Thickness of pellet

A= Area of pellet

CHAPTER 4



RESULTS AND DISCUSSIONS

4.1 Structural Characterization:

4.1.1 X-Ray Diffraction Analysis (XRD)

X-ray diffraction analysis is one of the important instrumental characterization which is able to identify the physical phases exists in bulk sample. In conventional ceramic method, the very first step is to get the phase pure powder once the first stage of heat-treatment is over. To get phase pure powder, calcination is done to develop the desired phase. Another thing should finally be checked regarding phase stability after sintering. XRD analysis enable us to make decision in both above mentioned cases.

4.1.1 [A] XRD pattern of calcined powders

The three batches which contains NiO, ZnO and Fe₂O₃ for target composition as Ni_{0.8}Zn_{0.2}Fe₂O₄ (here-after is coded as 'NZF') of mix with MnO₂ as additive 0.2, 0.4 and 0.6 in weight percentage were calcined at 950 °C/4hr to see the development of desired ferrite phase (NZF). The XRD patterns of calcined powder of four batches have been represented schematically in below.

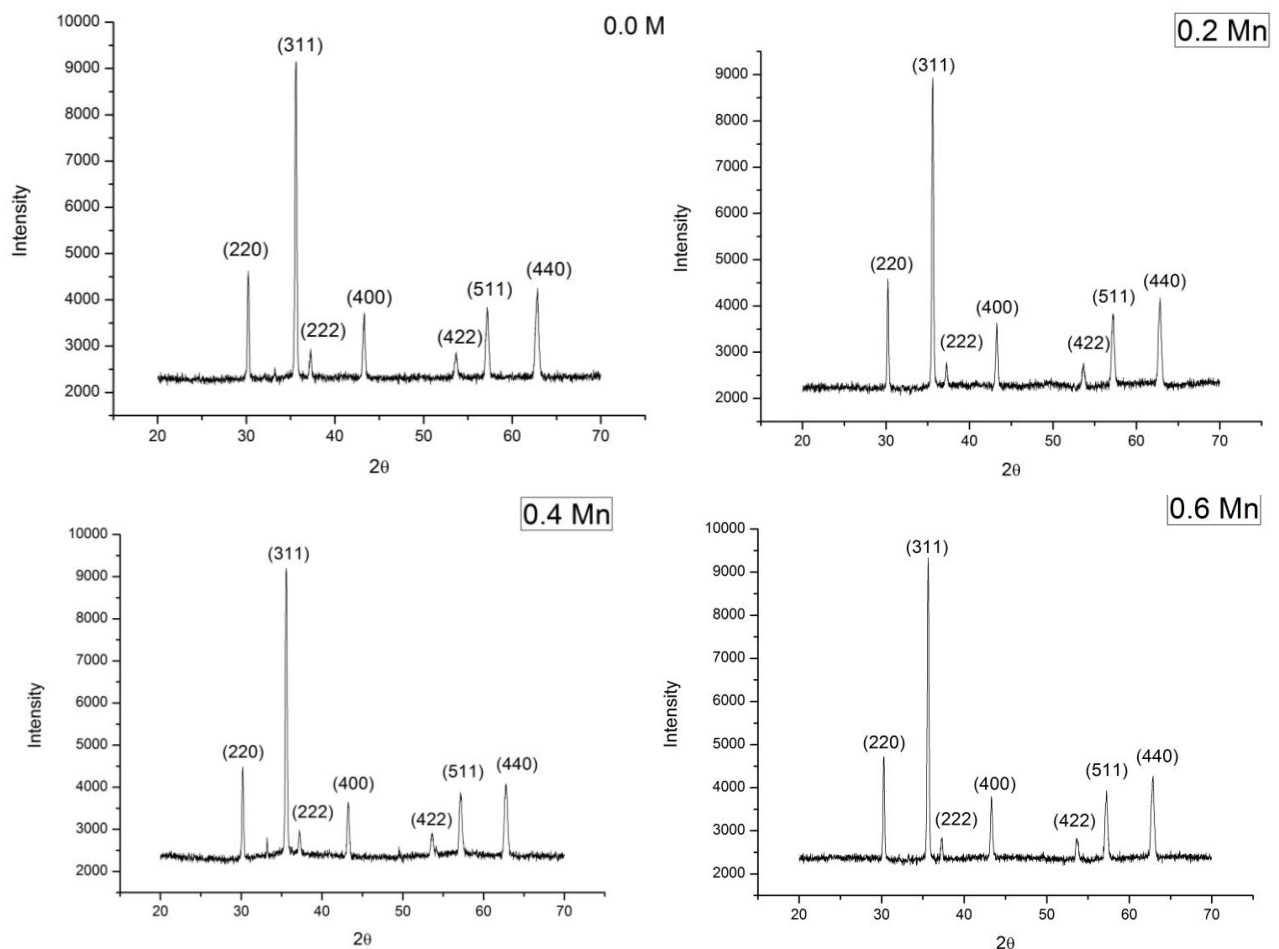


Fig. 4.1 XRD of calcined powder of batches containing (i)NZF+0.0MnO₂(ii) NZF+0.2MnO₂ (iii) NZF+0.4MnO₂ (iv) NZF+0.6MnO₂

From the figure 4.1 it was observed that there are a group of peaks conforms to spinel structure. The individual pattern has been matched with the reference pattern ...

The details of obtained information like peak position and *Full Width at Half Maxima* (FWHM) etc. have been given at table 4.1.

Table: 4.1 Table containing d-spacing, (hkl) plane and FWHM of calcined powder

Pos. [°2Th.]	d-spacing [Å]	FWHM [°2Th.]	(hkl) plane
30.8146	2.90176	0.1476	(220)
36.1895	2.48217	0.1968	(311)
37.8317	2.37812	0.1968	(222)
43.8418	2.06505	0.1476	(400)
54.2239	1.69165	0.1968	(422)
57.7416	1.59668	0.1968	(511)
63.3429	1.4671	0.24	(440)

It could be concluded that the calcination at 950 °C gives rise phase pure powder of ferrite.

4.1.1 [B] XRD pattern of sintered pellets

All calcined powders were compacted and sintered above 1200 °C/4hr. The polished surface of all sintered pellets were undergone X-ray Diffraction experiment. The XRD patterns were analysed in details to see the phase stability as well as crystallographic structural parameters. The patterns have been represented at figure below as per composition.

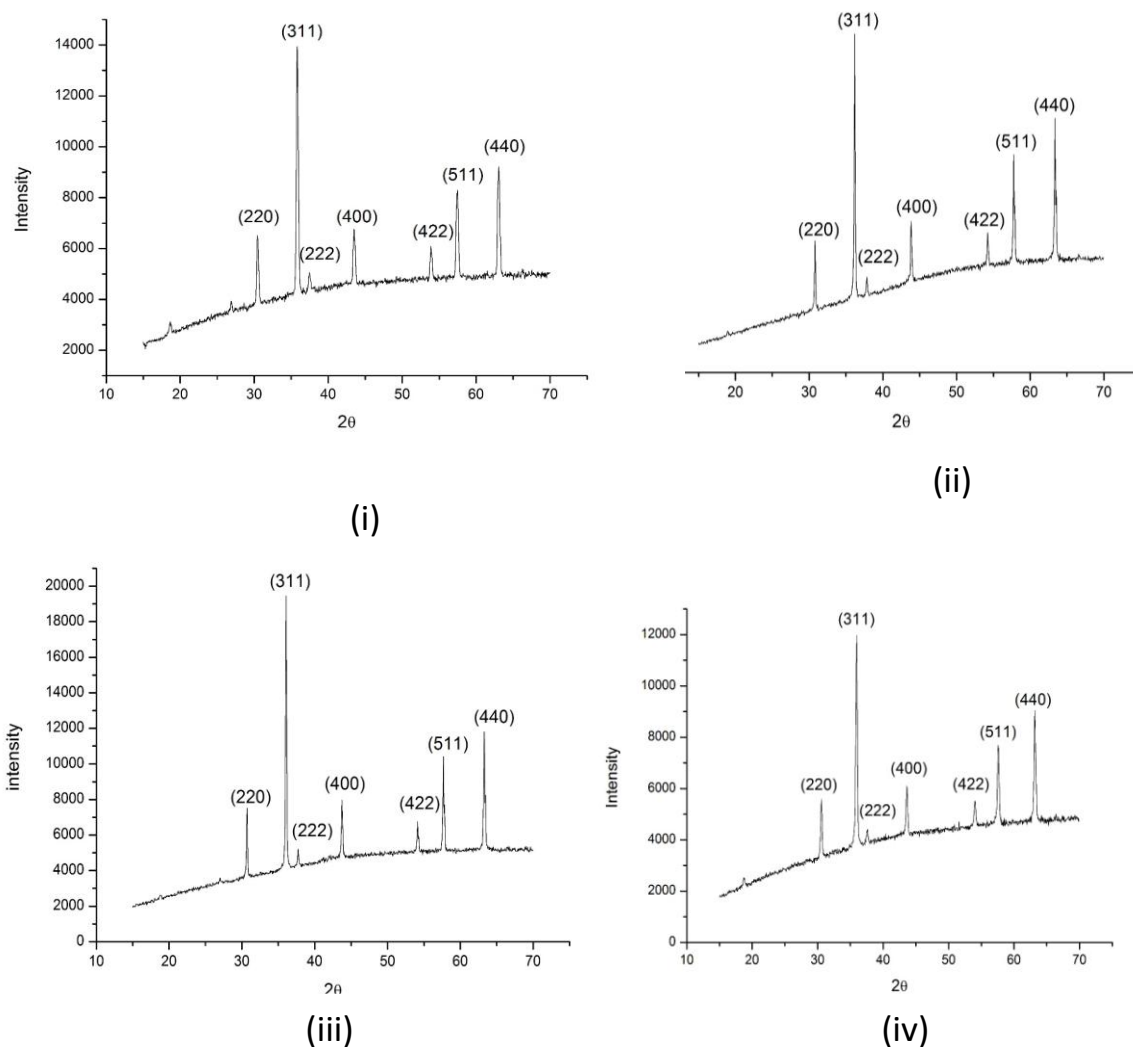


Fig 4.2 XRD of sintered pellets (i)NZF+0.0MnO₂(ii) NZF+0.2MnO₂ (iii) NZF+0.4MnO₂ (iv) NZF+0.6MnO₂

The obtained patterns were matched with the reference pattern no. 52-0277 from JCPDS database. Crystallite sizes of each batches were calculated by Scherer's formula that involves FWHM as one of the parameters. The results have been summarized at table 4.2 and table 4.3.

Table: 4.2 Table containing d-spacing, (hkl) plane of sintered pellets

Pos. [°2Th.]	d-spacing [Å]	FWHM [°2Th.]	(hkl) plane
30.5877	2.92277	0.1968	(220)
35.9701	2.49681	0.246	(311)
37.5743	2.39382	0.246	(222)
43.6232	2.07489	0.1968	(400)
54.053	1.69659	0.246	(422)
57.552	1.60149	0.246	(511)
63.1683	1.47074	0.3	(440)

Table: 4.3 Crystallite size as per composition sintering temperature = 1225 °C; dwell time = 4hr

Composition	Sintering Temperature (°C)	Lattice parameter	Crystallite size
NZF+0.0MnO ₂	1225	8.352	29.43
NZF+0.2MnO ₂	1225	8.349	28.36
NZF+0.4MnO ₂	1225	8.345	27.99
NZF+0.6MnO ₂	1225	8.341	20.96

Similar results have been reported by a group which showed lattice parameter comparable[10].

4.2 Microstructural Characterization:

Microstructures were analysed with the help of FESEM (Field Emission Scanning Electron Microscopy Technique). The samples were placed under the electron microscope.

4.2.1 Microstructure of sintered pellets at 1200 °C

The following figures shows the microstructure of different ferrite composition sintered at 1200 °C for 4 hours:

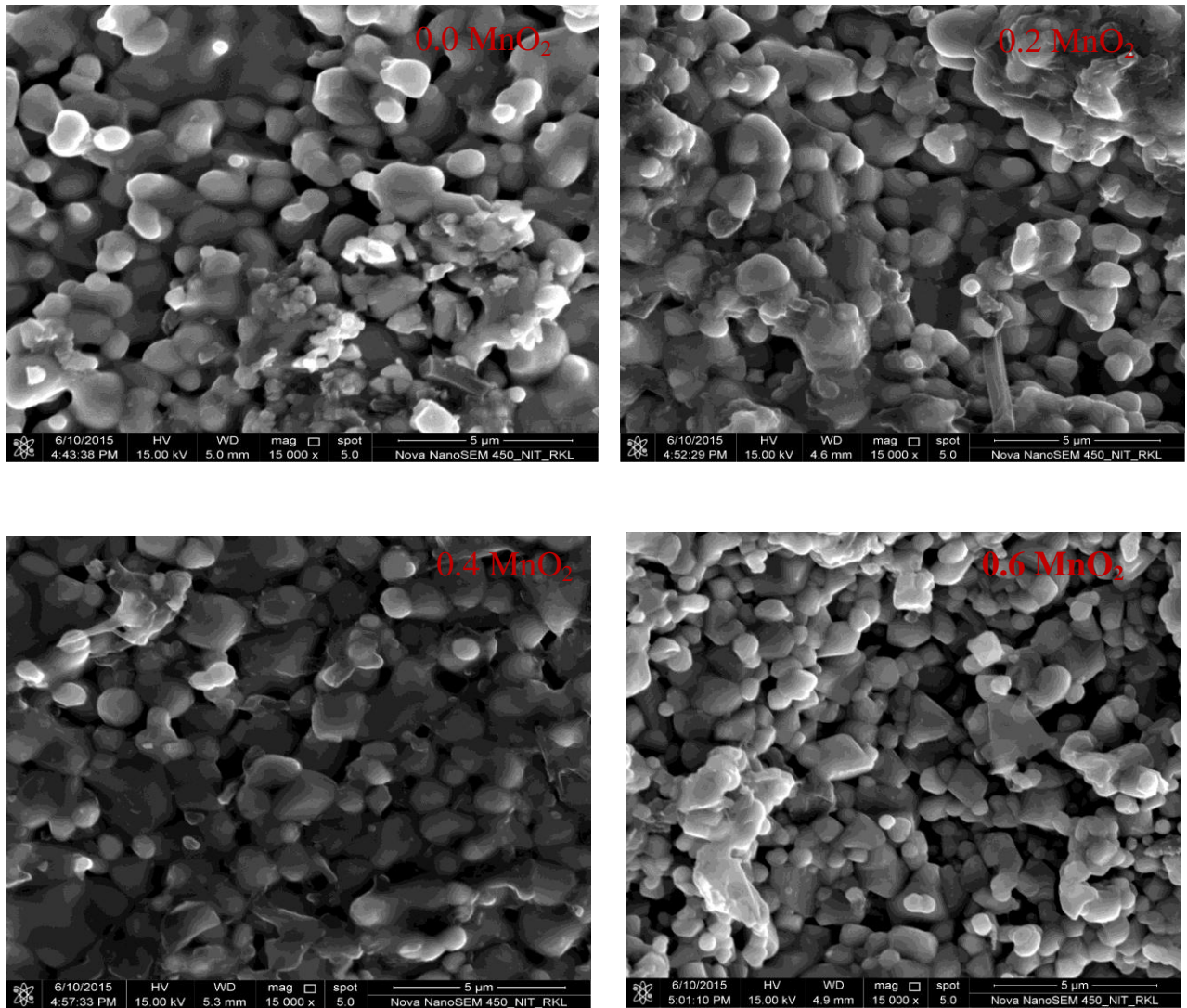


Fig 4.3 Microstructure of compositions of $\text{Ni}_{0.8}\text{Zn}_{0.2}\text{Fe}_2\text{O}_4$ sintered at $1200\text{ }^\circ\text{C}$ for 4hr (i)NZF+0.0MnO₂(ii) NZF+0.2MnO₂ (iii) NZF+0.4MnO₂ (iv) NZF+0.6MnO₂

From figure---it could be observed that appearance of NZF grains are mix of spherical and solid pyramidal shaped[11]. Grain sizes are not uniformly distributed but lies in a range. Grains with clear boundaries were found in each composition. The grain size ranges were divided into major three groups denoted as finer, intermediate and larger size. The average of three major sizes mentioned earlier were averaged statistically and given in table.

Microstructural informations are tabulated below where average grain sizes of three different size ranges were represented.

Table: 4.4 Average grain size of all four compositions sintered at 1200 °C for 4 hours

Composition	Grain size range(μm)	Average grain size(μm)
NZF+0.0MnO ₂	0.58-1.57	1.11
NZF+0.2MnO ₂	0.57-1.80	1.218
NZF+0.4MnO ₂	0.80-1.73	1.31
NZF+0.6MnO ₂	0.6-1.74	1.23

Elemental mapping were conducted with microstructural images taken in FE-SEM characterization. As the batch composition contained MnO₂ as additive (except NZF+0.0MnO₂), it was much of interest to see the distribution of Mn²⁺ ions throughout the sample. As many research groups came up with the fact that part of included MnO₂ in batch goes into the structure and a few remains at the grain boundary that modifies magnetic as well as electrical property. By elemental mapping one can predict whether significant amount of additive becomes a part of main crystal structure or remains as unreacted separate phase at grain boundaries. The following figure has been given to represent the addition of 0.02 weight percentage MnO₂ sintered sample at 1200 °C/4hr.

The elemental mapping of followings indicates that much of the MnO₂ went into basic structure rather than getting accommodation in grain boundaries. The effect could be well described by electrical and magnetic property as well.

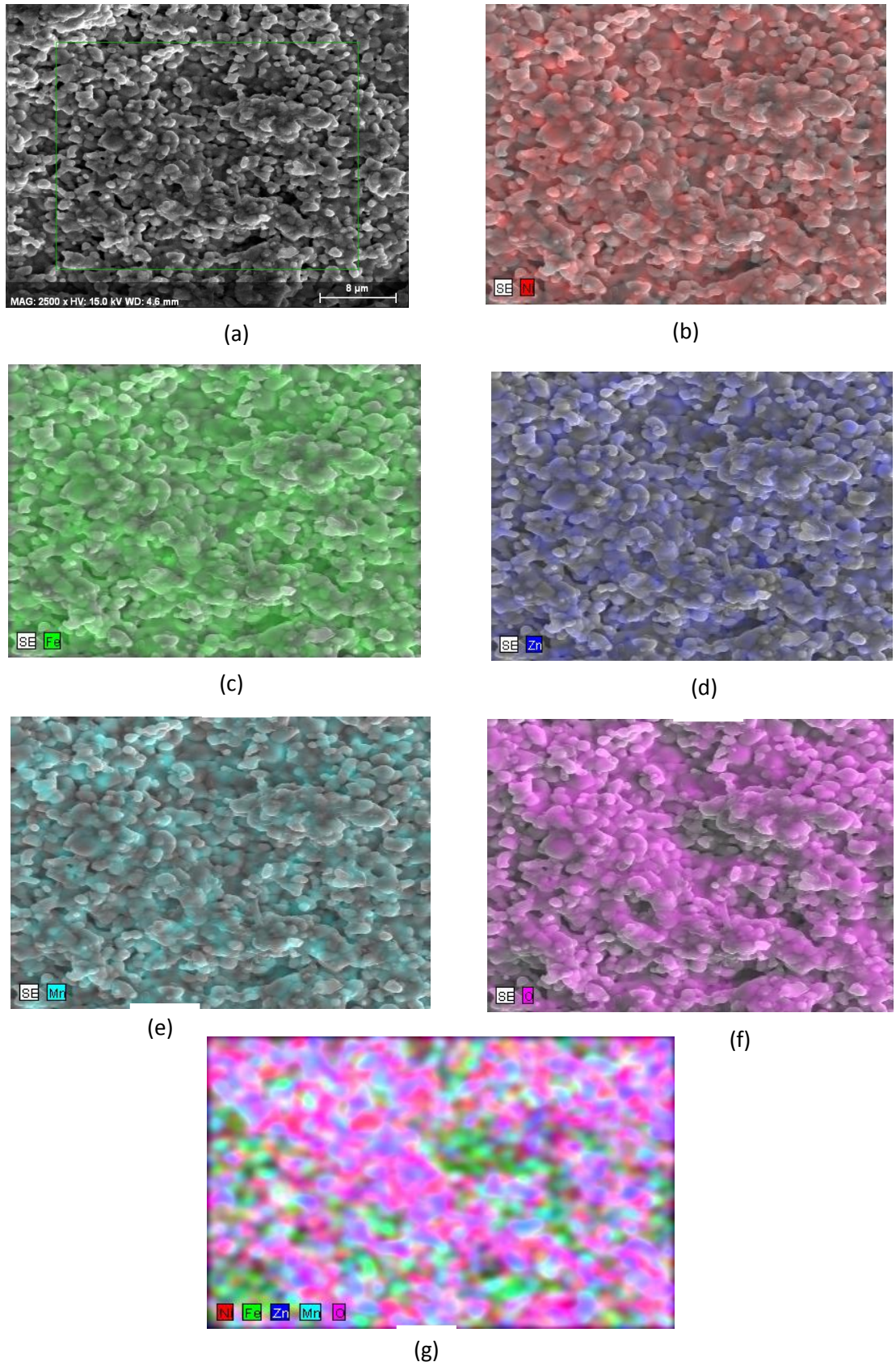


Fig. 4.4 Elemental mapping of NZF with 0.2 weight percentage MnO₂ additive sintered at 1200 °C/4hr (a) SE of NZF +0.2 MnO₂ (b) Ni (c) Fe (d) Zn (e) Mn (f) O (g) Ni,Zn,Fe,Mn,O

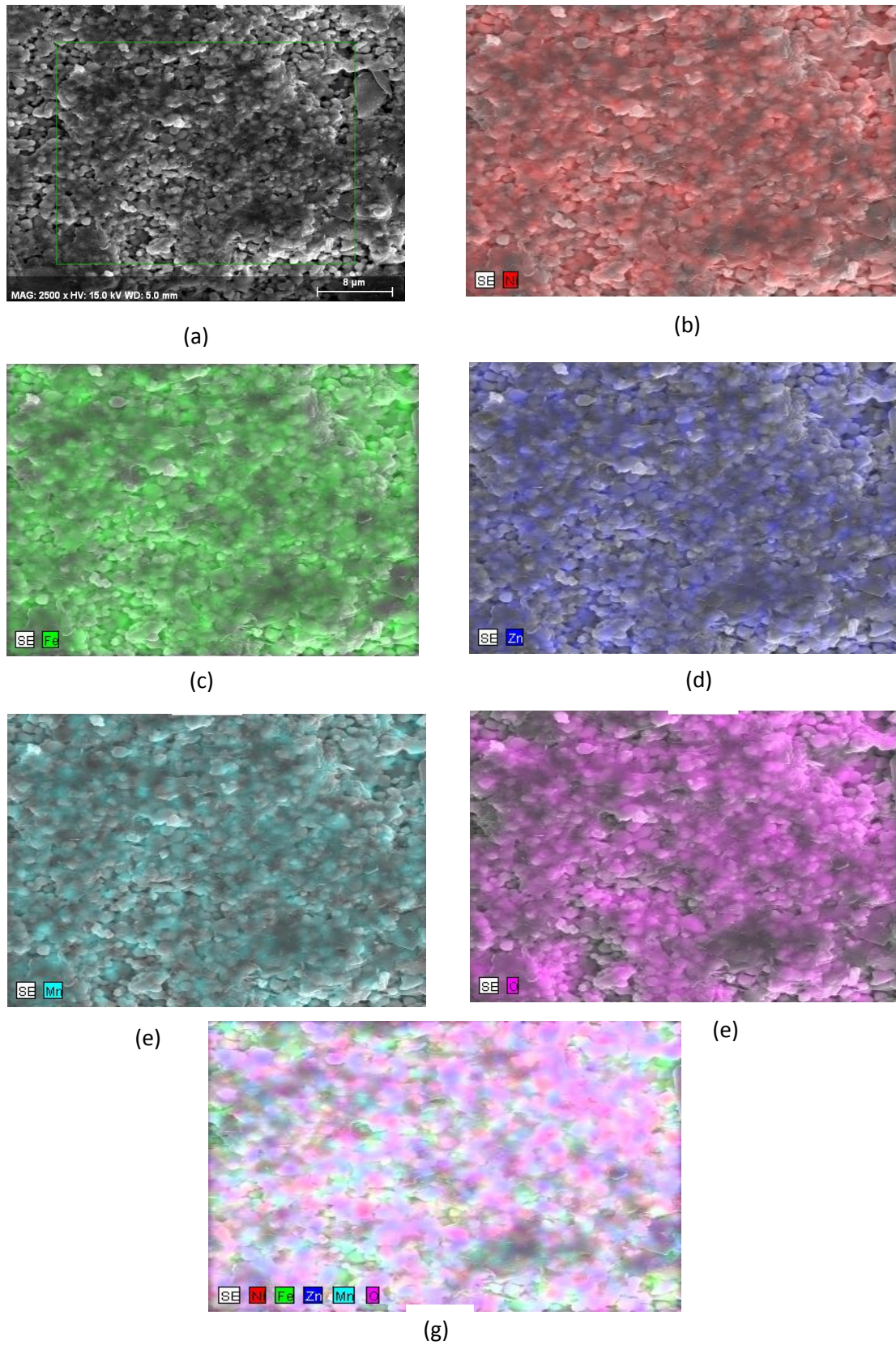


Fig. 4.5 Fig. 4.4 Elemental mapping of NZF with 0.2 weight percentage MnO_2 additive sintered at $1200\text{ }^\circ\text{C}/4\text{hr}$ (a) SE of NZF +0.2 MnO_2 (b) Ni (c) Fe (d) Zn (e) Mn (f) O (g) Ni,Zn,Fe,Mn,O

4.2.2 Microstructure of sintered pellets at 1225 °C

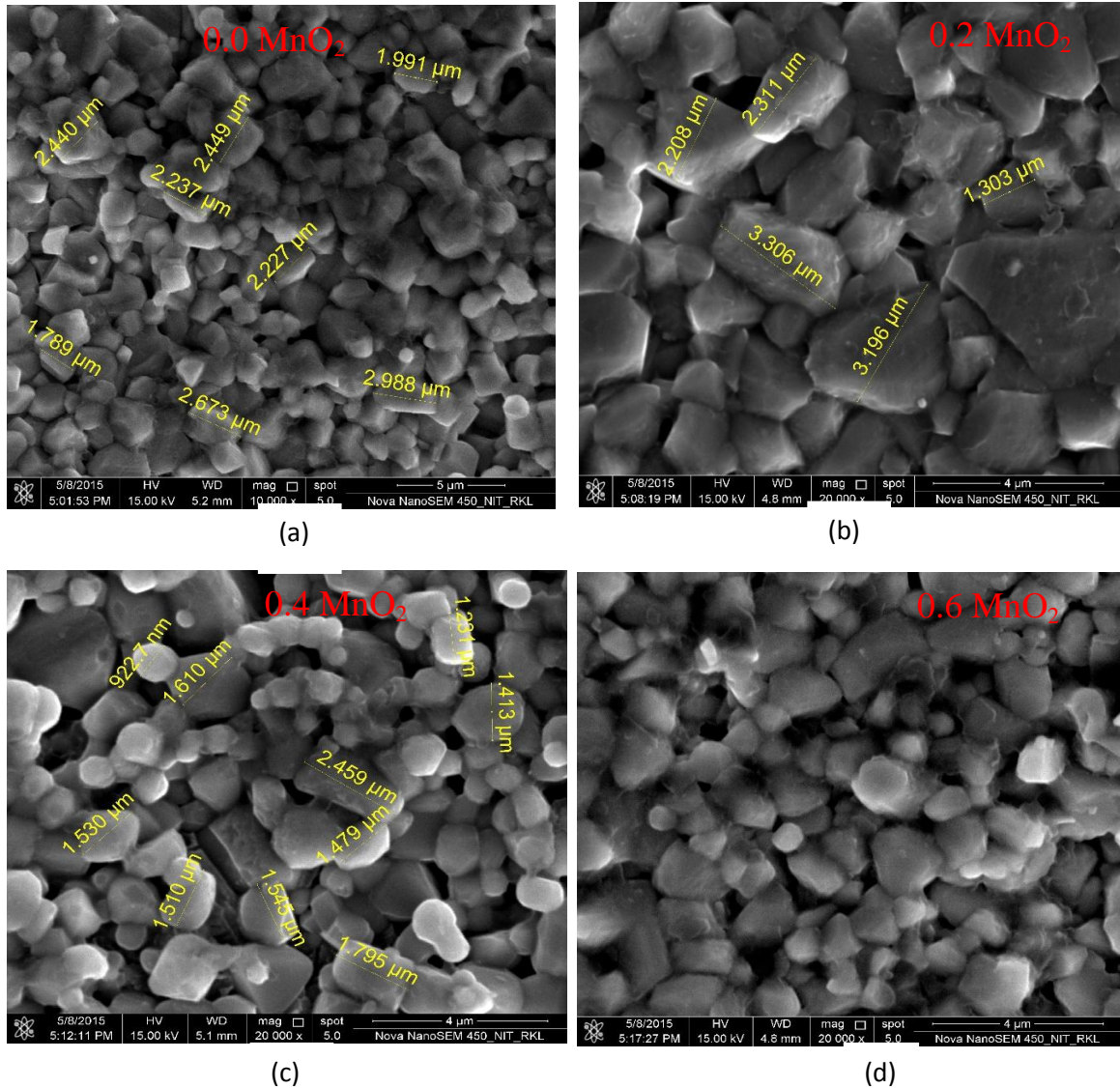


Fig. 4.6 Microstructures of all four compositions of NZF sintered at 1225 °C (i)NZF+0.0MnO₂(ii) NZF+0.2MnO₂ (iii) NZF+0.4MnO₂ (iv) NZF+0.6MnO₂

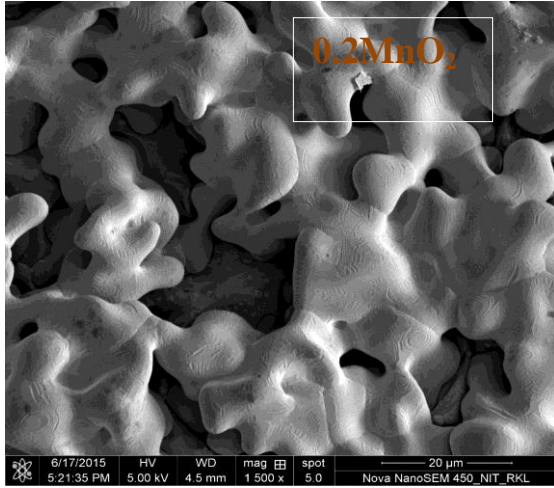
As represented at figure 4.6, the grains are distinguishable with sharp boundaries that indicate that thermal energy did not create deformation.

Table: 4.5 Average grain size of all four compositions sintered at 1225 °C for 2 hours

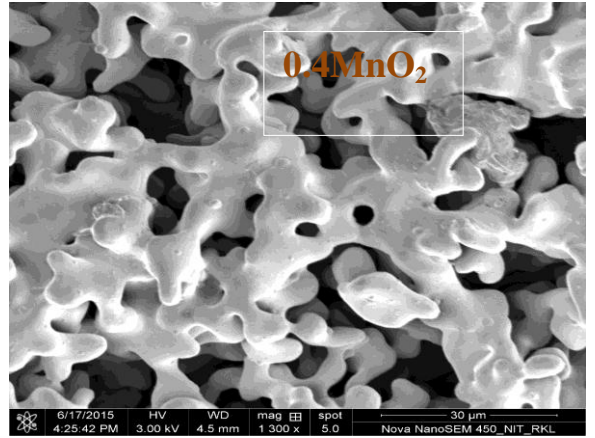
Composition	Grain size range(μm)	Average grain size (μm)
NZF+0.0MnO ₂	1.13-2.62	1.89
NZF+0.2MnO ₂	0.85-2.39	1.55
NZF+0.4MnO ₂	0.67-1.88	1.34
NZF+0.6MnO ₂	0.71-1.78	1.31

4.2.3 Microstructure of sintered pellets at 1225 °C in Argon atmosphere

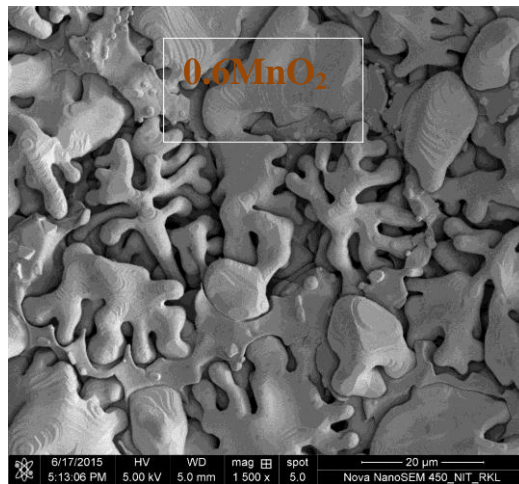
Number of research groups across the world have tried to enhance the electrical and magnetic properties by minimizing the oxygen vacancies created at high temperature while using air atmosphere[12]. The effort has been given much by replacing air-atmosphere with inert one. In this work, an attempt has also been taken to sinter the samples in inert atmosphere. The Following figure shows the microstructure of ferrite composition fired at 1225 °C for 2 hr.



(i)



(ii)



(iii)

Fig 4.7: Microstructures of all four compositions of NZF sintered at 1225 °C/2hr (inert atmosphere) (i) NZF+0.2MnO₂ (ii) NZF+0.4MnO₂ (iii) NZF+0.6MnO₂

As fig 4.7 represents, grains are found in melted condition which is evident from the running over to one from another. Sintering of that batches require temperature for heat-treatment should be lower than 1225 °C.

4.3 BULK DENSITY (B.D.)

Measurement of bulk density were carried out with applying *Archimedes principle*. The B.D. plays an important role in determining the desired properties that includes magnetic and electrical properties. The table 4.6 shows the percentage of theoretical density of Ni-Zn Ferrite with various sintering temperature. The tables given below contains the apparent porosity, bulk density and % of theoretical density of sintered samples. First group of pellets of all four compositions were sintered at 1200 °C. The soaking time for sintering was given as 4 hour.

Table: 4.6 Bulk density and apparent porosity value with % theoretical density of the ferrite having composition as $\text{Ni}_{0.8}\text{Zn}_{0.2}\text{Fe}_2\text{O}_4$, and $\text{Ni}_{0.8}\text{Zn}_{0.2}\text{Fe}_2\text{O}_4$ with MnO_2 in different amount as additive at 1200 °C for 4 hour

Composition	Bulk Density	Apparent porosity (%)	% of Theoretical Density
NZF+0.0MnO ₂	4.702	4.64	88.38
NZF+0.2MnO ₂	4.64	11.94	87.21
NZF+0.4MnO ₂	4.62	10.98	86.23
NZF+0.6MnO ₂	4.63	10.95	86.46

If percentage of theoretical density column is been seen that composition with addition of MnO₂ has less B.D. compared to Ni_{0.8}Zn_{0.2}ZnO₄ without MnO₂. That could be due to non-uniform distribution of temperature of furnace used for sintering of the pellets. Though further experiment necessary to prove the aforementioned statement. Presently it is considered that sintering of temperature should be lifted to an extent to get over all increased B.D.[13,15]. As the bulk density value is significantly less as compared to theoretical density of Ni_{0.8}Zn_{0.2}Fe₂O₄. So, the samples of each composition are then sintered at 1225 °C. The soaking time for the sintering is 2 hours.

Table: 4.7 Bulk density and apparent porosity value with % theoretical density of the ferrite having composition as $\text{Ni}_{0.8}\text{Zn}_{0.2}\text{Fe}_2\text{O}_4$ and $\text{Ni}_{0.8}\text{Zn}_{0.2}\text{Fe}_2\text{O}_4$ +varying MnO_2 as additive at 1225 °C for 2 hour

Composition	Bulk Density	Apparent porosity	% of Theoretical Density
NZF+0.0MnO ₂	5.046	0.88	94.84
NZF+0.2MnO ₂	5.042	2.8	94.77
NZF+0.4MnO ₂	4.941	3.7	92.87
NZF+0.6MnO ₂	4.876	4.2	91.65

Table: 4.8 Bulk density and apparent porosity value with % theoretical density of the ferrite having composition as $\text{Ni}_{0.8}\text{Zn}_{0.2}\text{Fe}_2\text{O}_4$ fired at 1225 °C for 4 hr

Composition	Bulk Density	Apparent porosity	% of Theoretical Density
NZF+0.0MnO ₂	4.876	4.04	91.65
NZF+0.2MnO ₂	4.82	6.08	90.60
NZF+0.4MnO ₂	4.875	2.47	91.63
NZF+0.6MnO ₂	4.67	11.37	87.78

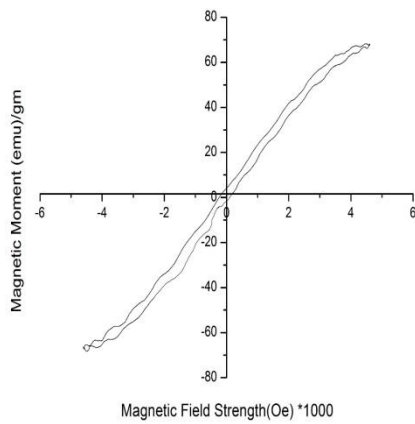
As represented B.D. and A.P. in table 4.6, 4.7 and 4.8 with corresponding sintering temperature as 1200 °C/2hr, 1225 °C/2hr, 1225/4hr, it could be concluded that 1225 °C/2hr sintered pellets should be given priority to observe the electrical and magnetic characteristics.

4.3 Magnetic and Electrical Properties:

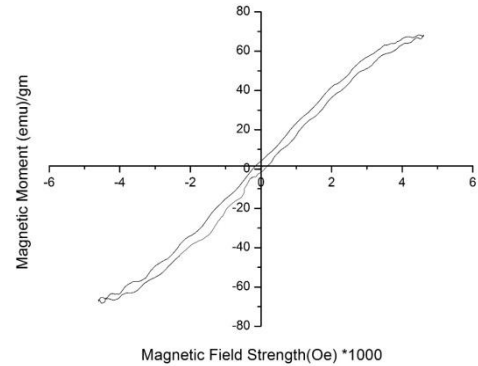
4.3.1 Magnetic properties

One magnetic hysteresis loop tracer was employed to see magnetic properties of the all batches prepared. As it has already been established that the increased B.D. improves both magnetic and electrical properties the B-H measurements were accomplished with samples with highest obtained B.D[15]. The following figure represents the typical magnetic loop characteristics.

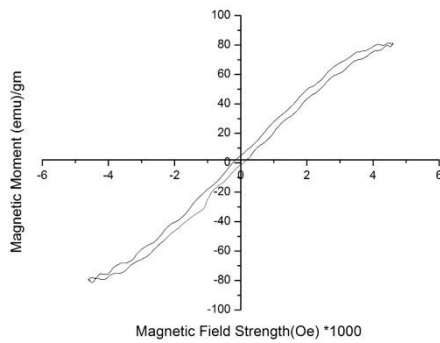
B-H loop of different compositions at 1225 °C for 2 hours has been represented in following figure:



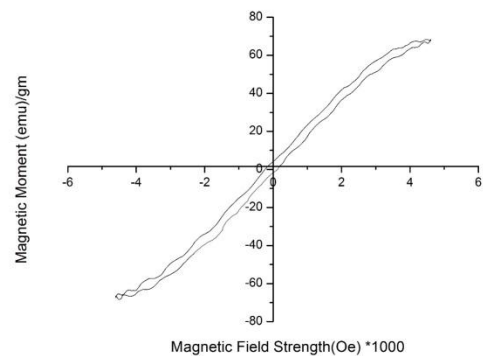
B-H loop of NZF+0.0% MnO₂



B-H loop of NZF + 0.2% MnO₂



B-H loop of NZF+0.4% MnO₂



B-H loop of NZF+0.6% MnO₂

Fig: 4.8 B-H loop at 1225 °C for 2 hours

B-H loop as represented at fig 4.8 exhibits typical magnetic behaviour as soft ferrites show commonly. The magnetization parameters are summarized and given in following table 4.9. Electrical resistivity at room temperature was measured with a sophisticated multimeter to measure resistance and resistivity subsequently.

Table: 4.9 Hysteresis parameters of Ni_{0.8}Zn_{0.2}Fe₂O₄ sintered at 1225 °C for 2 hours

Composition	Coercivity, Hc (Oe)	Remnant Magnetization, Mr (emu/g)	Saturation Magnetization, Ms (emu/g)	Electrical Resistivity (Ω-cm)
NZF+0.0MnO ₂	0.205	2.1	67.94	0.23×10 ⁸
NZF+0.2MnO ₂	0.210	4.70	79.80	1.09×10 ⁸
NZF+0.4MnO ₂	0.315	3.52	79.90	2.77×10 ⁸
NZF+0.6MnO ₂	0.325	3.63	68.21	19.11×10 ⁸

4.3.2 Electrical resistance at room temperature

Electrical resistivity is important as maximization of that property reduces the eddy-current loss. In that way, they are proved to be better in energy efficient inductor-core. As seen from table 4.9, in general the resistivity is higher in MnO₂ added composition compared to NZF without MnO₂.

As shown in tabulation, the magnetic properties are a little bit improved by the addition of MnO₂ possibly due to modified spinel structure after incorporation of MnO₂. [4].

Chapter 5



CONCLUSION

CONCLUSION

- Phase-pure $\text{Ni}_{0.8}\text{Zn}_{0.2}\text{Fe}_2\text{O}_4$ powder was obtained after calcination of mix oxide of Fe_2O_3 , NiO and ZnO_2 in required proportion at $950\text{ }^\circ\text{C}$ for 4hr.
- The sintering temperature of ferrite composition was optimized at $1225\text{ }^\circ\text{C}$ for 2 hour at normal atmosphere.
- Average grain size and sintering density gradually decrease with the increase of MnO_2 Content.
- DC resistivity is largely affected by additive MnO_2 and found to increase with the addition of MnO_2 Content.
- The saturation magnetisation increases with addition of MnO_2 Content.

REFERENCES:

1. Moulson A. J. and Herbert J. M., *Electroceramics Materials Properties Applications*, Wiley, 2003
2. Monica Sorescu, L. Diamandescu, R. Peelamedu, R. Roy, P. Yadoji, “Structural and magnetic properties of NiZn ferrites prepared by microwave sintering” 279 (2004) pp. 195-201
3. Purushotham Yadoji, Ramesh Peelamedu, Dinesh Agrawal and Rustum Roy, “Microwave sintering of Ni–Zn ferrites: comparison with conventional sintering” *Materials Science and Engineering B*. 98 (2003) pp. 269-278
4. R. V. Mangalaraja, S. Ananthakumar, P. Manohar, F. D. Gnanam and M. Awano, “Characterization of $\text{Mn}_{0.8}\text{Zn}_{0.2}\text{Fe}_2\text{O}_4$ synthesized by flash combustion technique” *Materials Science and Engineering A*. 367 (2004) pp. 301-305
5. R. V. Mangalaraja, S. Anantha kumar, P. Manohar and F. D. Gnanam, “Initial permeability studies of Ni–Zn ferrites prepared by flash combustion technique” *Materials Science and Engineering A*. 355 (2003) pp. 320–324
6. SU Hua, ZHANG Huai-wu, TANG Xiao-li, JING Yu-lan, “Microstructure and magnetic properties of Ni-Zn ferrites doped with MnO_2 ”, *Transactions of Nonferrous Metals Society of China* 21 (2011) 109-113.
7. S. S. Paik, S. J. Kim, Y. Shon, Hyunsik Im and H. S. Kim, “Study on Structural and Magnetic Properties of $\text{Ni}_{0.8}\text{Zn}_{0.2}\text{Fe}_2\text{O}_4$ ”, *Journal of the Korean Physical Society* 45 (2004) S637- S641.
8. Majid Niaz Akhtar, Noorhana Yahya, Patthi Bin Hussain, “structural and magnetic characterization of Nano structured $\text{Ni}_{0.8}\text{Zn}_{0.2}\text{Fe}_2\text{O}_4$ prepared by self combustion method”, *International Journal of Basic & Applied Sciences IJBAS-IJENS* (2009).
9. Tania Jahanbin,, Mansor Hashim, Khamirul Amin Matori, Samaila Bawa Waje, “Influence of sintering temperature on the structural, magnetic and dielectric properties of $\text{Ni}_{0.8}\text{Zn}_{0.2}\text{Fe}_2\text{O}_4$ synthesized by co-precipitation route”, *Journal of Alloys and Compounds* 503 (2010) 111–117.
10. M. Jalaly, M.H. Enayati, P. Kameli, F. Karimzadeh, “Effect of composition on structural and magnetic properties of nanocrystalline ball milled $\text{Ni}_{1-x}\text{Zn}_x\text{Fe}_2\text{O}_4$ ferrite”, *Physica B* 405 (2010) 507–512.
11. Hong-Wen Wang and Shong-Chung Kung, “Crystallization of nanosized Ni–Zn ferrite powders prepared by hydrothermal method”, *Journal of Magnetism and Magnetic Materials*. 270 (2004) pp. 230-236
12. C. Zhao, J. Vleugels, B. Basu and O. Van Der Biest, “HIGH TOUGHNESS Ce-TZP BY SINTERING IN AN INERT ATMOSPHERE”, *Scripta mater.* 43 (2000) 1015–1020

13. R. V. Mangalaraja, P. Manohar, F. D. Gnanam, “Electrical and magnetic properties of Ni_{0.8}Zn_{0.2}Fe₂O₄/silica composite prepared by sol-gel method”, JOURNAL OF MATERIALS SCIENCE 39 (2004) 2037 – 2042
14. P.A.Jadhav,R.S.Devan,Y.D.Kolekar,B.K.Chougule, “Structural, electrical and magnetic characterizations of Ni–Cu–Zn ferrite synthesized by citrate precursor method”, Journal ofPhysicsandChemistryofSolids70(2009)396–400.
15. M.A. Gabal, S. Kosa, T.S. Al Mutairi, “Structural and magnetic properties of Ni_{1-x}Zn_xFe₂O₄ nano-crystalline ferrites prepared via novel chitosan method”, Journal of Molecular Structure 1063 (2014) 269–273.